International Journal of Nanomedicine

Dovepress
open access to scientific and medical research

Open Access Full Text Article

ORIGINAL RESEARCH

Key Transdermal Patch Using Cannabidiol-Loaded Nanocarriers with Better Pharmacokinetics in vivo

Po-Cheng Chu[1,2], Man-Hua Liao[3], Mao-Gu Liu[1], Cun-Zhao Li[2], Ping-Shan Lai[1]

[1]Department of Chemistry, National Chung Hsing University, Taichung, Taiwan; [2]Basic Research and Development Department, Powin Biomedical Co. Ltd., Taichung, Taiwan; [3]Graduate Institute of Biotechnology, National Chung Hsing University, Taichung, Taiwan

Correspondence: Ping-Shan Lai, Department of Chemistry, National Chung Hsing University, No. 145, Xingda Road, Taichung, 402, Taiwan, Tel +886-4-22840411 Ext 428, Fax +886-4-22862547, Email pslai@email.nchu.edu.tw

International Journal of Nanomedicine downloaded from https://www.dovepress.com/
For personal use only.

Purpose: Cannabidiol (CBD) is a promising therapeutic drug with low addictive potential and a favorable safety profile. However, CBD did face certain challenges, including poor solubility in water and low oral bioavailability. To harness the potential of CBD by combining it with a transdermal drug delivery system (TDDS). This innovative approach sought to develop a transdermal patch dosage form with micellar vesicular nanocarriers to enhance the bioavailability of CBD, leading to improved therapeutic outcomes.

Methods: A skin-penetrating micellar vesicular nanocarriers, prepared using nano emulsion method, cannabidiol loaded transdermal nanocarriers-12 (CTD-12) was presented with a small particle size, high encapsulation efficiency, and a drug-loaded ratio for CBD. The skin permeation ability used Strat-M™ membrane with a transdermal diffusion system to evaluate the CTD and patch of CTD-12 (PCTD-12) within 24 hrs. PCTD-12 was used in a preliminary pharmacokinetic study in rats to demonstrate the potential of the developed transdermal nanocarrier drug patch for future applications.

Results: In the transdermal application of CTD-12, the relative bioavailability of the formulation was 3.68 ± 0.17-fold greater than in the free CBD application. Moreover, PCTD-12 indicated 2.46 ± 0.18-fold higher relative bioavailability comparing with free CBD patch in the ex vivo evaluation. Most importantly, in the pharmacokinetics of PCTD-12, the relative bioavailability of PCTD-12 was 9.47 ± 0.88-fold higher than in the oral application.

Conclusion: CTD-12, a transdermal nanocarrier, represents a promising approach for CBD delivery, suggesting its potential as an effective transdermal dosage form.

Keywords: cannabidiol, pharmacokinetics, transdermal, nano emulsion, drug patch, nanocarrier

Introduction

Cannabidiol (CBD) is a promising therapeutic drug with low addictive potential and a favorable safety profile.[1] Studies have shown that CBD does not exhibit the psychoactive effects commonly associated with tetrahydrocannabinol (THC), making it a safer option for therapeutic use. Its non-addictive nature makes it an appealing choice for patients seeking effective treatments without the risk of dependency. Clinical studies have indicated that CBD holds promise for potential applications in treating various chronic diseases and neurological conditions, with possible positive effects for managing conditions such as epilepsy,[2,3] Alzheimer's disease,[4] Parkinson's disease,[5,6] sleep disorders,[7,8] depression and psychotic disorders,[9] anxiety,[9] schizophrenia,[10] and post-traumatic stress disorder.[11] However, CBD has faced certain challenges affecting its administration and efficacy. One challenge has concerned its hydrophobic nature, with poor water solubility posing difficulties in formulating CBD into aqueous solutions, limiting its options for oral delivery.[12,13] Another disadvantage has been the low oral bioavailability of CBD. CBD undergoes extensive first-pass metabolism in the liver when taken orally, significantly reducing its bioavailability.[14,15] Hence, only a fraction of the orally administered CBD reaches the systemic circulation in an active form, reducing its therapeutic effectiveness. Despite these drawbacks, ongoing research has aimed to develop innovative strategies to improve CBD's solubility and oral bioavailability, including nano formulations and other delivery systems. These advancements may enhance the effectiveness of CBD as a therapeutic drug and expand its applications in various medical conditions.

Received: 14 December 2023
Accepted: 29 April 2024
Published: 16 May 2024

© 2024 Chu et al. This work is published and licensed by Dove Medical Press Limited. The full terms of this license are available at https://www.dovepress.com/terms.php and incorporate the Creative Commons Attribution – Non Commercial (unported, v3.0) License (http://creativecommons.org/licenses/by-nc/3.0/). By accessing the work you hereby accept the Terms. Non-commercial uses of the work are permitted without any further permission from Dove Medical Press Limited, provided the work is properly attributed. For permission for commercial use of this work, please see paragraphs 4.2 and 5 of our Terms (https://www.dovepress.com/terms.php).

Graphical Abstract

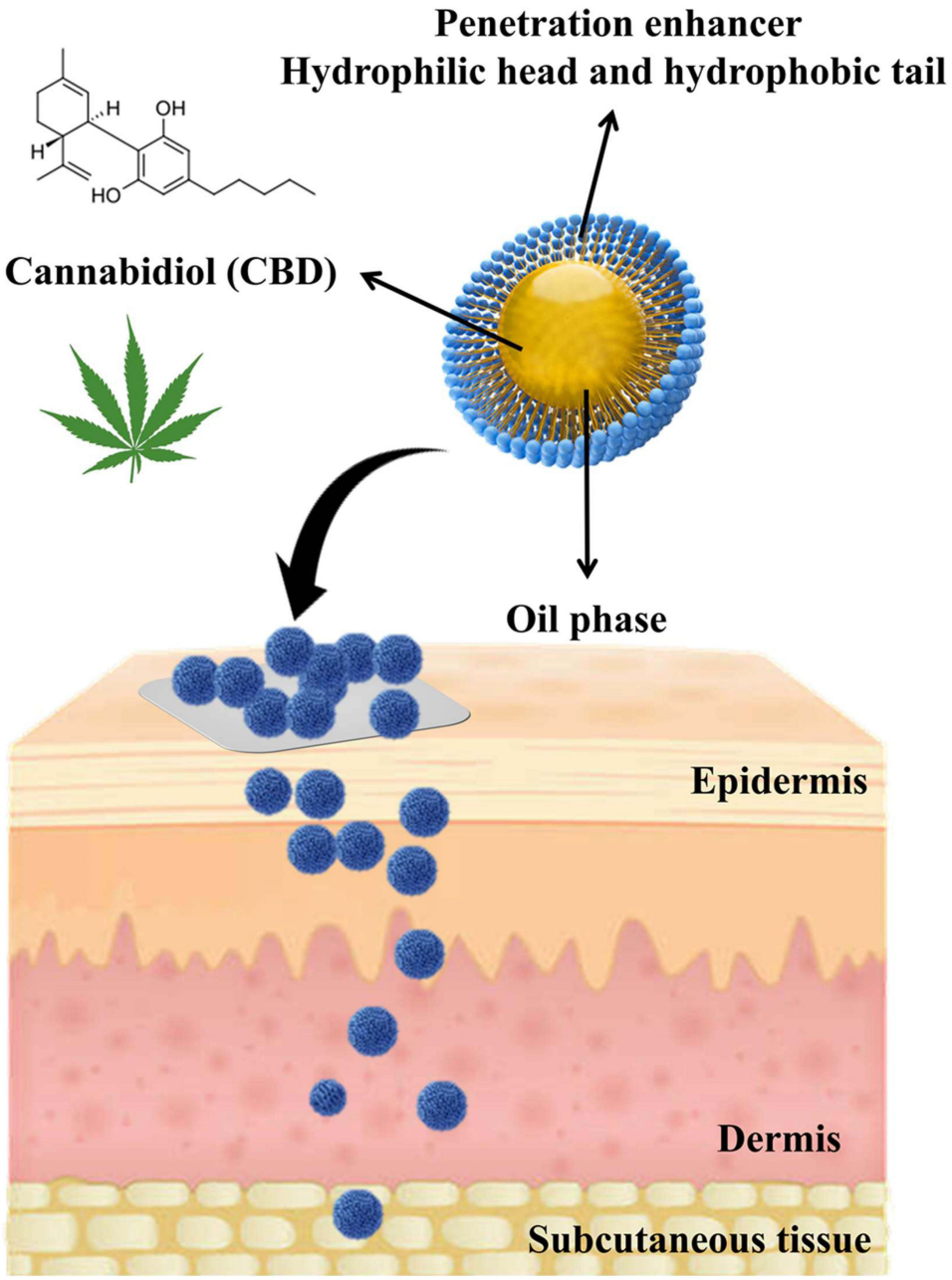

In the pharmaceutical industry, oral intake remains the most preferred method of drug administration due to its advantages, such as the availability of various dosage forms, painless administration, the feasibility of solid formulations, self-administration, and patient compliance.[16–18] However, oral drug delivery also has disadvantages, including drug stability in the gastrointestinal tract, first-pass metabolism, poor water solubility, and limited absorption through physiological barriers.[19,20] To address these drawbacks, transdermal drug delivery has emerged as a promising alternative. A transdermal drug delivery system (TDDS) utilizes the skin to administer therapeutic agents.[21,22] These agents permeate the skin, are absorbed into the blood vessels, and are distributed throughout the body.[23–25] TDDS offer non-invasiveness, minimal pain, first-pass metabolism bypassing, ease of administration, independence from medical

personnel, and potential applicability to a wide range of hydrophilic and hydrophobic drugs.[26–30] However, one limitation of transdermal drug delivery is the difficulty of drug penetration through the human skin, which is hard and resistant to infiltration.[31] The human skin comprises three main layers: the epidermis, dermis, and hypodermis. The low water concentration gradient from 75% in the viable epidermis to only 10–30% in the stratum corneum contributes to the lower permeability of molecules and drugs across the stratum corneum.[32]

In recent years, nanoparticle drug delivery systems in TDDS have shown significant potential for targeted drug delivery, increased drug stability, prolonged drug action, and improved bioavailability.[33–38] Several nanocarrier formulations have been developed to enhance transdermal drug delivery, including liposomes, ethosomes, transfersomes, polymeric micelles, self-nanoemulsifying drug delivery system (SNEDDS), solid lipid nanoparticles (SLN), nanostructured lipid carriers (NLCs), and polymeric nanoparticles.[39–44] Despite the growing popularity of TDDS, there have been limited developments in formulations specifically for CBD. Nanocarriers formulation provides a promising platform for enhancing the delivery of CBD. Indeed, encapsulating CBD within nanocarriers could overcome its limited solubility in water, improve stability, and potentially prolong its release. These nanocarriers could be designed to facilitate the penetration of CBD through the skin barrier, allowing for efficient absorption into systemic circulation. Thus, integrating this nanocarriers-based CBD formulation into a transdermal patch offers a synergistic approach to optimizing CBD delivery. The patch provides a convenient, non-invasive method for delivering CBD, while the nanocarriers formulation enhances its bioavailability by facilitating its permeation through the skin. This combined approach holds great potential for the treatment using of CBD.

Therefore, this study aimed to harness the potential of CBD by combining it with a TDDS. This innovative approach sought to develop a transdermal patch dosage form with micellar vesicularnanocarriers to enhance the bioavailability of CBD, leading to improved therapeutic outcomes. We aimed to address the challenges associated with CBD's hydrophobicity and low oral bioavailability by utilizing micellar vesicular nanocarriers technology combined with formulation materials skin-penetrating properties. Micellar vesicular nanocarriers demonstrated promise for enhancing the delivery of CBD. Thus, encapsulating CBD within nanocarriers could overcome its limited solubility in water, improve stability, and potentially prolong its release. These nanocarriers could be designed to facilitate the penetration of CBD through the skin barrier, allowing for efficient absorption into systemic circulation.

Materials and Methods

Materials included Strat-M membrane (Strat-M Membrane, Transdermal Diffusion Test Model, 25 mm, Merck, Darmstadt, Germany), d-limonene 97% (Sigma-Aldrich, USA), Tween 80 (Sigma-Aldrich, USA), cannabidiol (SCI Pharmtech, Inc., Taiwan), 2-acrylamido-2-methyl-1-propanesulfonic acid sodium salt solution (AMPS, Sigma-Aldrich, USA), N, N-methylene-bis-acrylamide (NMBA, Sigma-Aldrich, USA), hydroxyethyl cellulose (HEC, Sigma-Aldrich, USA), glycerol (Sigma-Aldrich, USA), diethylene glycol monoethyl ether (DEGME, Sigma-Aldrich, USA), and 2-hydroxy-2-methylpropiophenone (UVC-1173, TCI, Japan). All chemicals were of analytical grade and used without further purification.

Preparation and Characterization of Transdermal Nanocarriers

Transdermal nanocarriers were produced using a nano emulsion method of Tween 80 as the surfactant phase combined with limonene as the oil phase in different wt% (Table S1). After mixing the surfactant and oil phases at 50 °C 1000 rpm, we added D.D water inside and sonication with the condition of 600 W in ultrasonicator (Sonicator 3000, Misonix, Inc., New York, USA) for 30 min. The total weight of the solution was 1 g. After water addition, changes in sample appearance were visually monitored to determine if a precipitate, turbidity, or homogeneous solution was constituted.[45] The transdermal nanocarriers product are referred to as TD-NCs. The physical characterization of the developed TD-NCs used the dynamic light scattering (DLS) technique carried out by Malvern ZetaSizer Nano ZS (Malvern Instruments; Malvern, UK), and data were exported in Malvern Zetasizer Software v7.02.

Development and Characterization of CBD Loaded Nanocarriers

The method of preparing CBD loaded TD-NCs (CTD) was similar to preparing TD-NCs. First, 200 mg CBD was dissolved individually in 100 mg and 200 mg limonene and sonicated with the condition of 600 W in ultrasonicator (Sonicator 3000, Misonix, Inc., New York, USA) for 30 min. After achieving two groups of transparent solution, 400 mg and 100 mg of

Tween 80 were added individually at 50 °C 1000 rpm. Next, 500 mg and 700 mg of D.D water were added individually inside and sonicated with the condition of 600 W in ultrasonicator (Sonicator 3000, Misonix, Inc., New York, USA) for 30 min. The total weight of the solution was 1.2 g. Finally, CTD-41 was made from 200 mg CBD, 100 mg limonene, 400 mg Tween 80, and 500 mg D.D water, while CTD-12 was made from 200 mg CBD, 200 mg limonene, 100 mg Tween 80, and 700 mg D.D water. Samples were stored at 4 °C for further use. The physical characterization of CTD used the DLS technique by Malvern ZetaSizer Nano ZS (Malvern Instruments; Malvern, UK), and data were exported in Malvern Zetasizer Software v7.02. The morphology of the CTD was observed using high-resolution transmission electron microscopy (HR-TEM; Tecnai G2 20 STWIN). For the sample preparation of TEM imaging, the CTD were diluted 10-fold with 2%wt phosphotungstic acid. After mixing, 20 ul solution was dropped onto a 200 mesh formvar/carbon copper mesh (TED PELLA INC, USA) and dried using an oven at 37 °C before taking on HR-TEM.

The encapsulation efficiency (EE%) was measured and determined using HPLC and calculated using the Equation 1:

$$\text{Encapsulation efficiency}(\%) = \frac{W_{total} - W_{free}}{W_{total}} \times 100 \quad (1)$$

Where W_{total} means the initial weight of CBD added into the system and W_{free} means the weight of CBD did not in NPs. The drug loading (DL%) were measured with freeze-dried method and determined using HPLC and calculated using the Equation 2:

$$\text{Drug Loading}(\%) = \frac{W_{CBD\ in\ NPs}}{W_{NPs}} \times 100 \quad (2)$$

Where $W_{CBD\ in\ NPs}$ was the weight of CBD in formulation after being freeze-dried, and W_{NPs} was the dry weight of the formulation after being freeze-dried.

The HPLC analysis method was modified from previous studies.[46–48] Next, the appropriate standard of CBD was dissolved in MeOH diluted with MeOH to obtain solutions of known concentration, nine points in a concentration range between 0.98 and 250 μg/mL (ie, 0.98, 1.95, 3.91, 7.81, 15.63, 31.25, 62.50, 125.00, and 250.00 μg/mL). The standard solutions were stored away from light at −20 °C. The analysis was performed on an Agilent 1260 Infinity II LC System, consisting of a quaternary pump, a vials autosampler, a multicolumn thermostat column compartment, and a diode array detector (DAD). A ReproSil 100 C18 column (4.6 × 250 mm, 5 μm, Dr. Maisch GmbH, Germany) was used with the flow rate was set at 1 mL/min for 20 min and a mobile phase composed of 15% 0.5%-acetic acid and 85% MeOH. The column temperature was set at 30° C. The sample injection volume was 20 μL. The UV/DAD acquisitions were carried out in the 190–300 nm range, and chromatograms were acquired at 220 nm. Each group was prepared in triplicate, while the sample was previously filtered with a 0.22 μm PTFE filter.

Evaluation the Skin Permeation Ability of Nanocarriers

The skin permeation ability used Strat-M™ membrane with a transdermal diffusion system (DHC-6T, LOGAN Inc, USA).[1,49] Thus, 10 mg CBD and CTD containing the same weight CBD were added on the top of the Strat-M™ membrane. The diffusion experiment was initiated by charging the receiver compartment containing 6%wt Tween 80 in PBS for all groups. Besides, the free CBD group was using PBS to dispersed in donor receiver compartment. Three independent release experiments were conducted for each sample group, collecting full receiver solution and recharging fresh solutions at each time point: 0.5, 1, 2, 4, 6, 8, 12, and 24 hr. The collecting solutions were stored away from light at a temperature of 4 °C and filtered with a 0.22 μm PTFE filter before analysis in HPLC. At the final time point, the membrane was recollected and cut into pieces, adding 10 mL MeOH with sonication for 1 hr to elute the CBD inside the membrane for analysis. The HPLC analysis protocol for CBD was the same with we mentioned before in this study. Skin permeation ability data were plotted as the cumulative amount of drug collected in the receiver compartment as a function of time. Additionally, using the cumulative data and the equations, we calculated the flux (Equation 3), permeation ratio (Equation 4), release ratio (Equation 5), area under the curve (AUC, Equation 6), and relative formulation availability (FA, Equation 7) of each group:

$$\text{Flux}_{\ 0-24\text{hr}}\left(\frac{\text{mcg}}{\text{hr}\times\text{cm}^2}\right)=\frac{C_{CBD}}{t_{number}\times Area_M} \tag{3}$$

$$\text{Permeation ratio}(\%)=\frac{C_{CBD}}{\text{Total CBD}}\times 100 \tag{4}$$

$$\text{Release ratio}(\%)=\frac{C_{CBD}+M_{CBD}}{\text{Total CBD}}\times 100 \tag{5}$$

$$AUC_{0-24}(\text{mcg}\cdot\text{hr})=\frac{(C_{CBD1}+C_{CBD2})\times(t_{number2}-t_{number1})}{2} \tag{6}$$

$$FA(\text{fold})=\frac{AUC_{0-24\ \text{group}}}{AUC_{0-24\ \text{Free CBD}}} \tag{7}$$

where C_{CBD} was the cumulative CBD content at each time point during 24 hr, t_{number} was the time point during 24 hr, $Area_M$ was the diffusion area between the membrane and donor compartment, M_{CBD} was the CBD content in Strat-M™ membrane, and AUC_{0-24}.was the area under curve during 24 hr.

Loaded CTD-12 into AMPS Gel Formulation

CTD-12 loaded AMPS gel formulation used a mixing and UV-curing method. Thus, 0.5 g NMBA was dissolved in 25 g AMPS solution and gently stirred. Next, 9.5 g glycerol was mixed and dispersed with 0.5 g HEC at 50 °C, followed by adding 9 g D.D water inside. Finally, the two solutions were mixed at room temperature to acquire the AMPS pre-mixture. The pre-mixture was stored away from light at a temperature of 4 °C for further use. In order to find the optimal ratio of CTD-12 loaded AMPS gel, we tried different combination parameters of AMPS pre-mixture with or without CTD-12 by fixing the photo initiator UVC-1173 (0.5 wt%) and co-solvent DEGME (4.5 wt%) at 5wt% in total formulation. Subsequently, the AMPS mixed with X wt% CTD-12 are referred to as CTD-12-X%. The optimal ratio is based on water content, contact angle, and gel curing appearance. The following uses the optimized formulation as a production example to illustrate the preparation steps. Subsequently, 5 g CTD-12 was mixed with 4.5 g AMPS pre-mixture at 800 rpm with 0.45 g DEGME added inside. Next, 0.05 g UVC-1173 was added inside the solution and stirred at 300 rpm while avoiding light and bubbles. The mixed solution was evenly coated on a glass slip and UV-curing (OPAS XLite 500, Taiwan) the sample for 45 sec. Next, the water content and contact angle of the sample were measured using a moisture analyzer (Sartorius MA37, Goettingen, Germany) and a contact angle meter (First Ten Angstroms 1000B, Newark, the USA). Subsequently, the optimized mixed solution was evenly coated on a melt-blown cloth with a manual coating rod at a thickness of 700 um. Finally, UV-curing (OPAS XLite 500, Taiwan) was applied to the sample at 45 sec and cut into 4 cm^2 (2*2 cm). The preparation patch was stored in a dry, light-proof location for future use. The patch was cut into pieces, adding 10 mL MeOH with sonication for 1 hr to elute the CBD inside the patch for analysis. The HPLC analysis protocol for CBD was the same with we mentioned before in this study. Subsequently, the terms prototype CTD-12 loaded AMPS gel patch are referred to as PCTD-12. Moreover, the free CBD AMPS patch were prepared and analyzed in the same protocol by using 1 mL MeOH dissolve CBD and mixing with D.D water to adjust the same wt% to PCTD-12.

Evaluation the Skin Permeation Ability of PCTD-12

The evaluation experiment of skin permeation ability for transdermal patch was the same protocol with we mentioned before in this study. Briefly, Free CBD patch and PCTD-12 were added on the top of the Strat-M™ membrane. The diffusion experiment was initiated by charging the receiver compartment containing 6%wt Tween 80 in PBS for all groups. Three independent release experiments were conducted for each sample group, collecting full receiver solution and recharging fresh solutions at each time point: 0.5, 1, 2, 4, 6, 8, 12, and 24 hr. The collecting solutions were stored away from light at a temperature of 4 °C and filtered with a 0.22 μm PTFE filter before analysis in HPLC. At the final time point, the membrane was recollected and cut into pieces, adding 10 mL MeOH with sonication for 1 hr to elute the CBD inside the membrane for analysis. The HPLC analysis protocol for CBD was the same with we mentioned before in this study. Skin permeation ability data were plotted as the cumulative amount of drug collected in the receiver compartment as a function of time. Additionally,

using the cumulative data and the equations, we calculated the flux (Equation 3), permeation ratio (Equation 4), release ratio (Equation 5), AUC (Equation 6), and FA (Equation 7) of each group.

In vivo Pharmacokinetic Evaluation

The animal study was conducted according to the guidelines of the Animal Care Committee of the National Chung Hsing University and approved by the Committee (IACUC No. 111–127) and performed in accordance with the National Research Council's Guide for the Care and Use of Laboratory Animals. Specific-pathogen-free male Wistar rats aged 6 weeks were purchased from BioLASCO (licensed by Charles River, Taiwan) per the Animal Ethics Committee of IACUC registration IACUC No. 111–127. For the pharmacokinetic study, seven rats were used: four for the oral route (Oral 10 mg CBD) and 3 for PCTD-12. During the experiment, each animal was housed in a standard laboratory cage and raised separately under the following conditions: controlled temperature, 25 °C ± 2 °C; humidity, 30–70%; light/dark cycle, 6 a.m. lights on/6 p.m. lights off; and access to water and standard diet, ad libitum. The animals were acclimatized to the animal facility for 1 week. On the day before the experiments were conducted, the abdomen was shaved, with the shaved area as the constant section of the entire abdomen 2 cm below the forelimbs and 1 cm above the hind limbs.

A PCTD-12 patch was applied to the abdomen and fixed with an elastic bandage. At the time points of 0.5, 1, 2, 4, 8, 12, and 24 hr, 0.2 mL of blood was collected in 1 mL micro blood collection tubes for subsequent serum extraction analysis. Following blood collection for 24 hr, all rats were sacrificed under gas anesthesia. The blood was centrifuged at 6000 rpm and 4 °C for 2 min immediately after collection, and the serum was extracted and stored at –80 °C until used for CBD extraction.

The CBD extraction step was modified from the reference.[50–52] First, 20 μL 10M KOH was added to 100 μL serum and heated at 70 °C for 30 min, subsequently adding 5 μL formic acid left standing for 5 min. Next, 625 μL of ACN was added, mixed well, and ultrasonicated for 30 min, then centrifuged at 5000 G, 4 °C for 5 minutes. After completion, the supernatant was extracted and stored in a –20 °C refrigerator. After removing the supernatant, the underlying pellet was added to 625 μL of ACN and extracted twice, resulting in 1875 μL of extracted samples at each time point. The standard curve was prepared with the CBD stock solution, a concentration of 1 mg/mL (1000 ppm) in ACN, and diluted to the concentration range of 5000–9.76 ppb. The plasma standard curve was prepared with the following protocol: adding 100 μL of blank serum in a micro tube, then adding 500 μL of CBD standard solution prepared in ACN in a range of 5000–9.76 ppb. After mixing for 1 min, the preparation was sonicated for 30 min and centrifuged at 4 °C, 5000 G for 5 min. Subsequently, the supernatant was extracted and stored in a –20 °C refrigerator. After removing the supernatant, the underlying pellet was added to 500 μL of ACN and extracted twice, resulting in 1500 μL of extracted plasma standard samples of different concentrations.

The CBD concentration in plasma was analyzed using LC-MS/MS from the extracted samples. LC-MS/MS analyses were modified from the reference and performed on the Liquid Chromatograph-Tandem Mass Spectrometer TSQ Altis (Thermo Scientific, CA, United States).[52–58] Samples were analyzed on an XBridgeTM C18 column (2.1 × 100 mm; 3.5 μm particle size; Waters, Ireland). The mobile phase was composed of (A) 0.2% formic acid and (B) acetonitrile using the following gradient program: 0.0–0.2 min, 25% (B); 0.2–4.0 min, linear gradient from 25 to 100% (B); 4.0–4.2 min, 100% (B); 4.2–4.3 min, linear gradient from 100 to 25% (B); and 4.3–10.0 min, 25% (B). The flow rate was 0.2 mL/min, and the column temperature was 25 °C. The injection volume was 5 μL, and the injector needle was washed with methanol while the autosampler was maintained at room temperature.

The chromatographic conditions were optimized by analyzing the standard solutions and extracts of whole blood spiked with the target analytes. Analytic software was used for instrument control, data acquisition, and qualitative and quantitative data analyses. Detection and quantitation of all serum-extracted samples used a single reaction monitoring mode (SRM) due to the high selectivity and sensitivity. Optimized instrument settings were as follows: ionization mode, negative; sheath gas, 35 arb; aux gas, 7 arb; sweep gas, 0 arb; ion spray voltage, 2500 V; ion transfer tube temperature, 325 °C; vaporizer temperature, 275 °C. Quantification was performed using the transition m/z 313.4–245.1 (CE = 23 V, 100 msec) and the second transition 313.4–179.1 (CE = 20 V, 100 msec) for CBD with a retention time of 5.8 min. Pharmacokinetics data were plotted as the plasma concentration of CBD extracted from the serum as a function of time. Additionally, the data in the equations were used to calculate each group's area under the curve of PK ($AUC_{PK\ 0–24}$, Equation 8) and relative bioavailability (BA, Equation 9):

$$\mathrm{AUC_{PK0-24}(ng/ml \cdot hr)} = \frac{(P_{CBD1} + P_{CBD2}) \times (t_{number2} - t_{number1})}{2} \quad (8)$$

$$\text{Relative bioavailability} = \mathrm{BA(fold)} = \frac{\mathrm{AUC_{0-24\ group}/Dose_{group}}}{\mathrm{AUC_{0-24\ Oral}/Dose_{Oral}}} \quad (9)$$

where P_{CBD} was the plasma concentration of CBD extracted from serum at each time point during 24 hr, t_{number} was the time point during 24 hr, and $Dose_{group}$ was the group dosage.

Results and Discussion

Various ratios of the oil phase and surfactant were tested to develop TD-NCs. The best composition for loading with CBD was selected based on the appearance of the solution, size, and PDI of TD-NCs. Limonene, a hydrocarbon lipophilic terpene, was chosen as the oil phase due to its high compatibility with CBD, solubility properties, and enhanced penetration abilities.[59–61] Tween 80, a nonionic surfactant known to enhance skin penetration,[62,63] was selected as the surfactant. The ability of these materials to enhance skin penetration arose from their interaction with and incorporation into stratum corneum components, which led to the disruption of the skin barrier function and an increase in skin interface permeability.[64] The ternary phase diagram in Figure 1 shows a combination of limonene, Tween 80, and D.D water used to determine the homogeneous range. The mixing conditions and steps to reach equilibrium were consistent for all mixtures. After equilibration, the mixtures were visually assessed for transparency, covering the entire phase region. In the diagram, the red area represents the milky range, the light gray area represents the precipitate region, and the dark gray area represents the turbidity region.

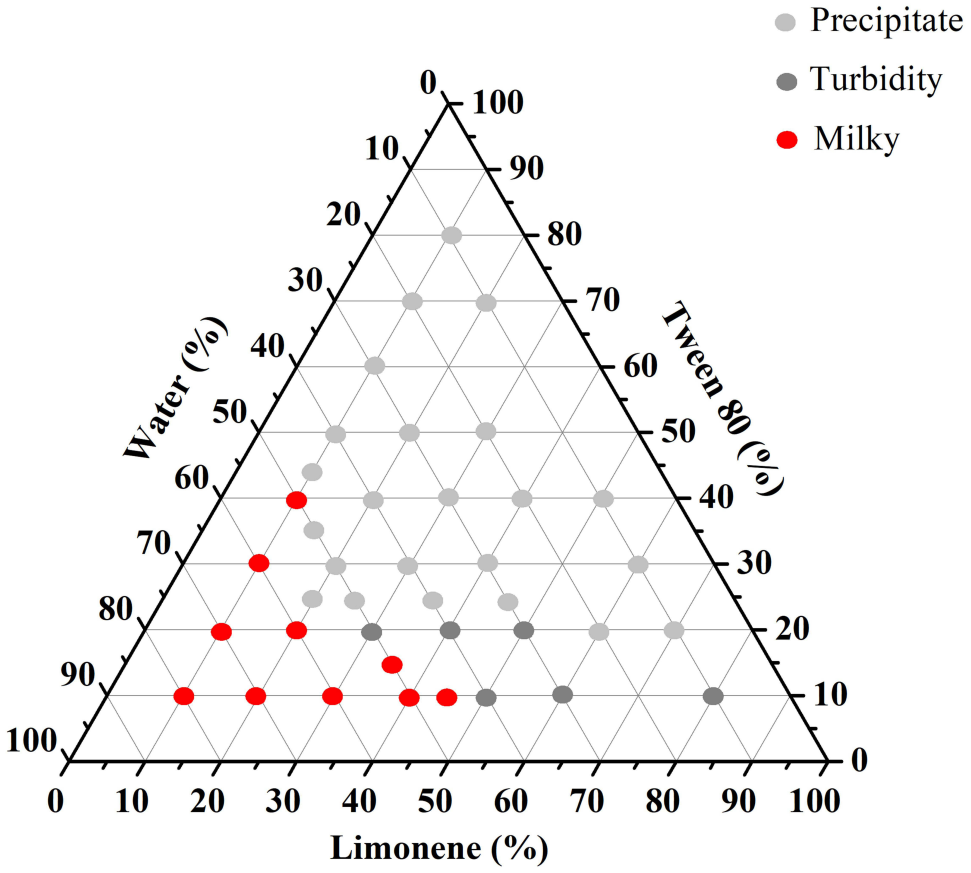

Figure 1 Ternary phase diagram. Light grey area represents the precipitate region, while the dark grey area represents the turbidity. Red area represents the milky region. Tween 80 = surfactant, Limonene = oil phase.

Moreover, the appearance of TD samples is shown in Figure S1. The selection of TD-NCs was based on the presence of homogeneously dispersed, hydrodynamic size, and PDI data. Table S2 overviews the appearance and DLS results of TD-NCs. Homogeneous appearance was observed in the range of 1:1.25 to 1:4 of Tween 80 to limonene weight percent (T:L). However, the size, PDI and Zeta potential of the solution did not exhibit a consistent pattern in response to changes in the T:L composition. One of the selected TD-NCs (TD-41) consisted of 40% Tween 80, 10% limonene, and 50% D.D water. Although TD-41 had higher PDI and higher zeta potential than others, it had the smallest hydrodynamic size among all the groups due to the high ratio of Tween 80. Another selected TD-NP (TD-12) was chosen based on the best PDI, the most negative zeta potential and smaller hydrodynamic size among all the groups. It consisted of 10% Tween 80, 20% limonene, and 70% D.D water. The developed TD-NCs were loaded with 16.66% CBD (total weight of CBD in solution / total weight of solution). CBD was dissolved in limonene and mixed, followed by sonication with Tween 80 and D.D water. Adding CBD decreased the PDI for both selected TD-NCs formulations, indicating increased uniformity of TD-NCs due to CBD's high compatibility with limonene. The higher DL% in CTD-12 was attributed to its higher limonene composition ratio, offering good solubility for CBD.

Figure 2A and B showed the TEM images of both CTD. As shown in Figure 2A, CTD-41 exhibited a morphology resembling a micellar system, attributed to its higher emulsifier ratio, consistent with previous report.[61] Interestingly, CTD-12 displayed a uniformly spherical shape, suggesting a self-assembled system (Figure 2B), similar with studies by Zhu et al and Lu et al[65,66] This may be attributed to the hydrophobic properties of limonene and CBD, leading to a stronger cohesive effect when emulsified with Tween 80, resulting in a more spherical appearance (Figure 2C). Additionally, from the TEM images of CTD, it can be inferred that the particle aggregation ability of CTD-41 and CTD-12 may vary. Factors influencing this phenomenon stem from the surfactant's capability within the formulation. Surfactants can potentially lower interfacial tension, providing space and electrostatic repulsion to prevent particle agglomeration and stabilize the emulsion.[67,68]

The above experiments demonstrated that due to the differences in T:L ratios, CTD-12 and CTD-41 had different morphologies and sizes. Therefore, the potential application of CTD as a transdermal formulation was further explored. The transdermal ability of CTD through artificial skin membranes was quantified using a transdermal diffusion system with a Strat-M^{TM} membrane, which has been widely used in transdermal diffusion testing.[69–72] The receiver channel was filled with a 6% wt% Tween 80 solution in PBS, which provided suitable sink conditions during the assays and was compatible with the skin membranes. The total amount of CBD in all groups was fixed at 10 mg, and the CBD concentration in the receiver channel was measured at different time points.

Figure 3A shows the 24-hr cumulative in vitro permeation CBD curves for the free CBD, 6% Tween 80, and CTD. The flux and permeation ratio of the drug permeated through the Strat-M^{TM} membrane at the end of 24 hr for all groups are

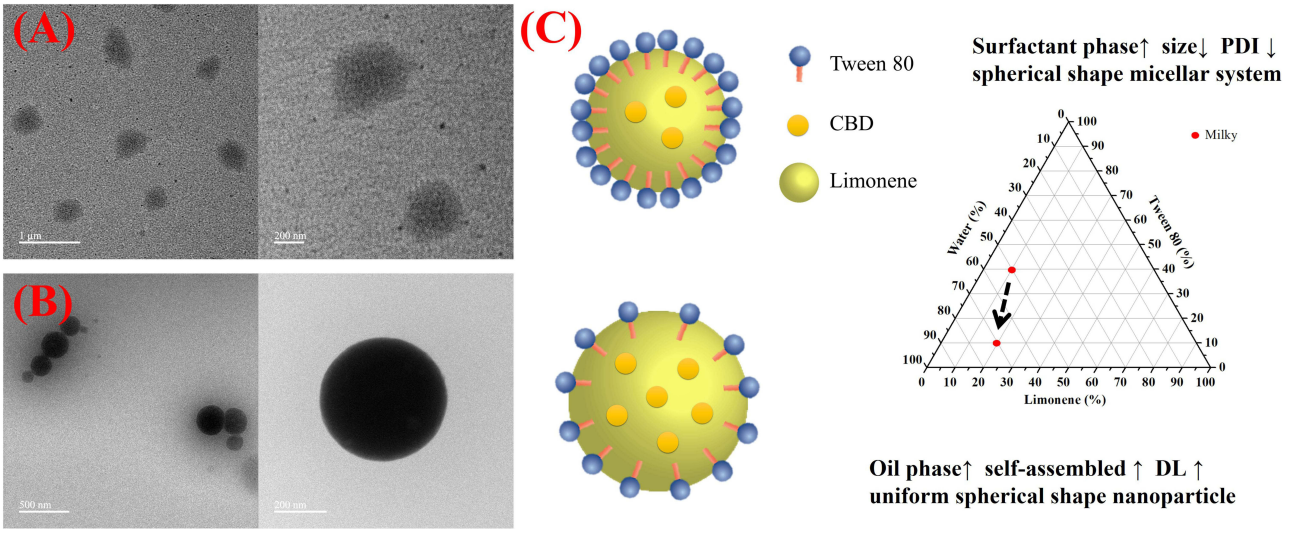

Figure 2 Morphology of different nano emulsion transdermal nanoparticle by TEM. (**A**) CTD-41. (**B**) CTD-12. (**C**) Schematic of the structural difference between CTD-41 and CTD-12. Arrows indicate the direction of change in formulation ratio.

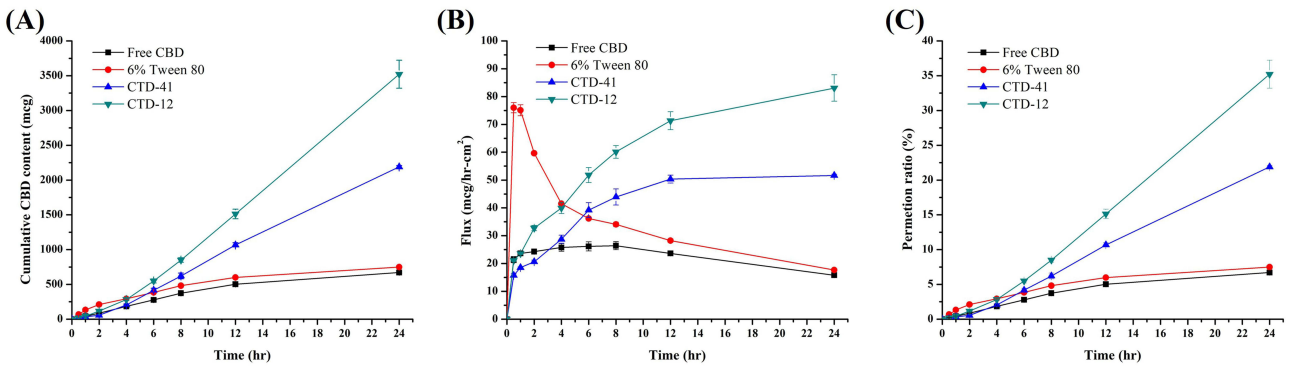

Figure 3 (**A**) Cumulative CBD content (**B**) Flux (**C**) Permeation ratio of Free CBD, 6% Tween 80, CTD-41 and CTD-12 during 0–24 hr at skin permeation experiment.

provided in (Figure 3B and C), respectively. Table 1 presents the numerical results of skin penetration from 0–24 hr for all groups. In the initial period of the skin permeation test, the Tween 80 group exhibited faster penetration and higher flux than the other groups within 2 hr, which was attributed to its chemical properties.[62–64] However, a significant increase in total CBD content was observed after changing the formulation into transdermal nanoparticles (CTD). These phenomena occurred due to the presence of Tween 80 and Limonene, which reduced the skin's barrier function by dissolving the lipid bilayer of the stratum corneum and enhanced the penetration ability of CBD into the skin interface.[61,62,64,73] CTD-41 began to exceed the free CBD curve at 4 hr and exceeded the 6% Tween 80 curve at 6 hr, while CTD-12 exceeded the free CBD curve at 1 hr and the 6% Tween 80 curve at 6 hr. Moreover, the $AUC_{0\text{-}24hr}$ of CTD-41 and CTD-12 was higher than the $AUC_{0\text{-}24hr}$ of the free CBD and the 6% Tween 80 groups. Surprisingly, the relative flux enhancement factors (FA) of CTD-41 and CTD-12 compared to the free CBD group were 2.43 ± 0.04-fold and 3.68 ± 0.17-fold, respectively, indicating their significant potential for future applications. Furthermore, CTD-12 performed better than CTD-41 in cumulative CBD content, flux and permeation ratio from 0–24 hr. In Table S3, we compared previous research on various CBD nano formulations and examined patent results related to CBD's transdermal capabilities. Whether it was the use of CBD with penetration enhancers alone or in a gel combined with CBD and penetration enhancers, CTD-12 consistently demonstrated superior performance compared to these patents.[74–77] When compared to other nano formulation systems, such as transfersome, NLC and so on, CTD-12 still indicated higher performance.[78–82] Therefore, CTD-12 was chosen as a promising transdermal formulation for further prospective application use in transdermal drug patches.

AMPS, a monomer used in superabsorbent hydrogels, proved suitable for establishing hydrogel interconnections and was chosen for use in this research.[83–85] The focus here was on maximizing the content of CBD, representing the optimal mixing ratio of CTD-12 and AMPS. In addition to drug content, criteria for judging the selection included gel appearance, UV curing integrity, contact angle, and water content. Figure S2 displayed the curing appearance, water content, and contact angle of

Table 1 Numerical Results of 0–24 hr Skin Permeation for Free CBD, 6% Tween 80, CTD-41 and CTD-12

Group	Free CBD	6% Tween 80	CTD-41	CTD-12
Dose (mcg)	10,000			
24 hr cumulative CBD content (mcg)	669.89 ± 8.92	747.94 ± 13.45	2189.76 ± 18.61	3521.45 ± 200.86
Membrane content (mcg)	73.07 ± 20.77	230.43 ± 8.31	1043.46 ± 29.59	1400.05 ± 45.14
Total CBD (mcg)	742.97 ± 29.69	978.37 ± 21.76	3233.22 ± 27.14	4921.50 ± 234.61
Release ratio (%)	7.43 ± 0.27	9.78 ± 0.19	32.33 ± 0.27	49.21 ± 2.35
Permeation ratio (%)	6.7 ± 0.09	7.48 ± 0.13	21.9 ± 0.19	35.21 ± 2.01
$Flux_{0\text{–}24hr}$(mcg/hr·cm^2)	15.8 ± 0.21	17.64 ± 0.31	51.66 ± 0.44	83.07 ± 4.74
$AUC_{0\text{-}24hr}$(mcg·hr)	10,234.09 ± 195.88	12,518.72 ± 160.11	24,886.41 ± 403.14	37,647.43 ± 1696.35
0–24 hr Relative FA (fold)	1	1.22 ± 0.02	2.43 ± 0.04	3.68 ± 0.17

Abbreviations: $AUC_{0\text{-}24hr}$, area under the curve-time curve from 0 to 24-hour time point, $Flux_{0\text{-}24hr}$, flux-time curve from 0 to 24-hour time point, FA, formulation bioavailability, CBD, Cannabidiol, CTD, Cannabidiol loaded transdermal nanocarriers.

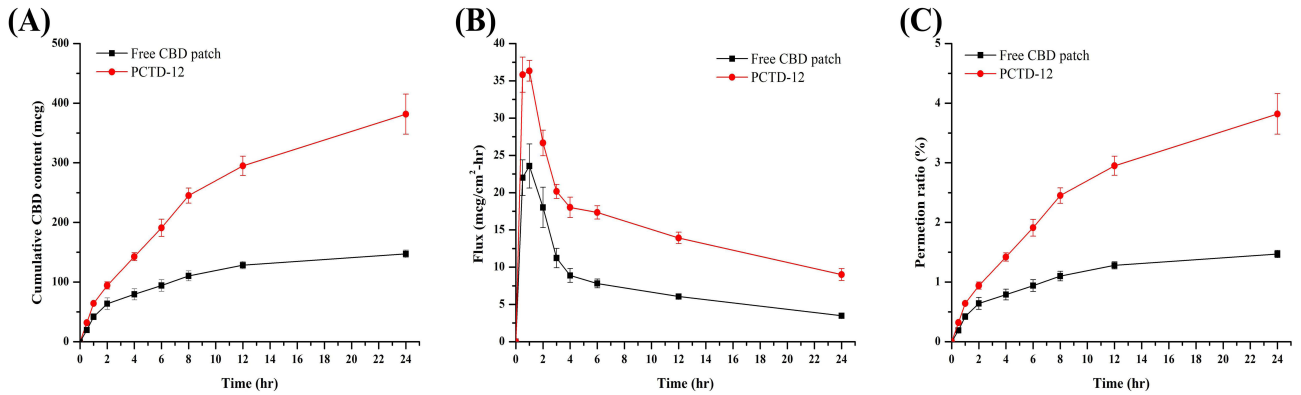

Figure 4 (**A**) Cumulative CBD content (**B**) Flux (**C**) Permeation ratio of Free CBD patch and PCTD-12 during 0–24 hr at skin permeation experiment.

different ratios of AMPS hydrogel mixed with CTD-12. As the water ratio in the formulation increased, the contact angle decreased, water content increased, and the AMPS hydrogel maintained a transparent appearance. However, when changing the distilled water into CTD-12, the appearance of the CTD-12-AMPS hydrogel became milky and not transparent. Most importantly, as the CTD-12 ratio increased to 60%, the gel would not cure completely. This indicated that CTD-12-50% was the best mixing ratio, composed of 50% CTD-12, 45% AMPS pre-mixture, 4.5% co-solvent, and 0.5% photo initiator. Subsequently, to cure the CTD-12-AMPS hydrogel into a specific shape, melt-blown cloth was chosen as the base material to support the shape. The prototype CBD-loaded transdermal nanocarrier drug patch was referred to as PCTD-12.

The above experiments demonstrated the optimal mixing ratio of CTD-12 and AMPS hydrogel and finally produced the prototype transdermal nanocarrier drug patch PCTD-12. Therefore, the potential of PCTD-12 as a transdermal drug patch was further explored. The transdermal ability of PCTD-12 through artificial skin membranes was quantified using the same method as we mention in this study before. (Figure 4A) shows the 24-hr cumulative in vitro permeation CBD curves for the free CBD patch, and PCTD-12. The flux and permeation ratio of the CBD permeated through the Strat-M^{TM} membrane at the end of 24 hr for the free CBD patch and PCTD-12 are provided in (Figure 4B) and (Figure 4C), respectively. Table 2 presents the numerical results of skin penetration from 0–24 hr for the free CBD patch and PCTD-12. In the initial period of skin permeation testing, PCTD-12 exhibited faster permeation and higher flux than the free CBD patch within 4 hr, and it still retained a certain penetration capacity after 4 hours. Within 24 hr permeation testing, PCTD-12 demonstrated the better performance than free CBD patch, which is due to the ability of the CTD-12 nanocarrier. These results indicated the potential of PCTD-12 as a transdermal nanocarrier drug patch for CBD.

Table 2 Numerical Results of 0–24 hr Skin Permeation for Free CBD Patch and PCTD-12

Group	Free CBD patch	PCTD-12
Dose (mg / patch)	8.47 ± 0.68	9.15 ± 1.02
24 hr cumulative CBD content (mcg)	147.25 ± 6.29	381.68 ± 33.5
Membrane content (mcg)	74.01 ± 1.77	668.85 ± 62.82
Total CBD (mcg)	221.26 ± 7.23	1050.53 ± 96.32
Release ratio (%)	2.62 ± 0.13	11.51 ± 0.28
Permeation ratio (%)	1.47 ± 0.06	3.82 ± 0.34
$Flux_{0\text{-}24hr}$ (mcg/hr·cm^2)	3.47 ± 0.15	9.00 ± 0.79
$AUC_{0\text{-}24hr}$ (mcg·hr)	1652.95 ± 76.36	4059.66 ± 297.71
0–24 hr Relative FA (fold) (Based on free CBD patch)	1	2.46 ± 0.18

Abbreviations: $AUC_{0\text{-}24hr}$, area under the curve-time curve from 0 to 24-hour time point, $Flux_{0\text{-}24hr}$, flux-time curve from 0 to 24-hour time point, FA, formulation bioavailability, CBD, Cannabidiol, PCTD, patch of cannabidiol loaded transdermal nanocarriers.

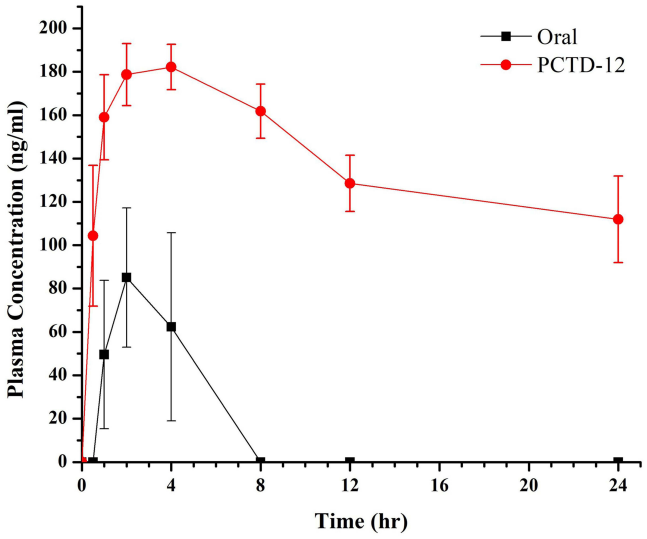

Figure 5 Plasma concentration curve of oral and PCTD-12 for 0–24 hours.

PCTD-12 was used in a preliminary pharmacokinetic study in rats to demonstrate the potential of the developed transdermal nanocarrier drug patch for future applications. The mean plasma concentration-time profiles of oral administration CBD at a dose of 10 mg per rat and PCTD-12 in one patch per rat are presented in Figure 5. Additionally, the numerical results of the 0–24 hr plasma concentration curve for oral and PCTD-12 administrations are summarized in Table 3. The pharmacokinetic parameters in rats exhibited several differences among the oral and PCTD-12 groups. In contrast to PCAS-12 groups, the Oral group showed lower C_{max}, cumulative CBD concentration, and AUC values. Notably, PCTD-12 exhibited significant potential in the transdermal route, with a relative bioavailability (based on oral administration) of 9.47 ± 0.88-fold, higher than the oral group. The parameters and plots obtained in this study were similar to more recently reported findings.[57,58,86] However, few pharmacokinetic studies have been reported for CBD in rats, particularly through the IV or Oral route.[57,58,86–89] Notably, PCTD-12 increased the plasma concentration of CBD during the 0–4 hr period. After 4 hr, PCTD-12 maintained plasma concentrations above 100 ng/mL for up to 24 hr. This sustained release phenomenon was due to the transdermal nanocarrier (CTD-12) in the patch, allowing for penetration through the skin. Tables S4 compare research and patent results regarding CBD transdermal ability and pharmacokinetics.[50,90–92]

In general, larger nanoparticles (size > 200 nm) encounter difficulty in penetrating the skin barrier and delivering the carried drug into the bloodstream, with the primary challenge lying in the ineffective permeation through the stratum corneum barrier.[93,94] Moreover, in non-nano carrier systems, surfactants cause a greater lipid disorientation effect in the stratum corneum and result in higher levels of cutaneous absorption compared to terpenes and solvents.[95] Increasing the concentration

Table 3 Numerical Results of 0–24 Hr Plasma Concentration Curve of Oral and PCTD-12

Group	Oral	PCTD-12
Dose (mg)	10	10.33 ± 1.67
C max (ng/mL)	85.77 ± 31.71	189.91 ± 3.80
T max (hr)	2 ± 0	3.33 ± 0.94
0–8hr cumulative (ng)	4338.77 ± 2412.88	17,336.41 ± 4256.51
0-24hr cumulative (ng)	4338.77 ± 2412.88	22,396.94 ± 5791.13
AUC 0–8 hr (ng/mL·hr)	351.96 ± 173.94	1309.54 ± 70.05
AUC 0–24 hr (ng/mL·hr)	351.96 ± 173.94	3332.90 ± 310.97
0–24 hr Relative BA (fold)	1	9.47 ± 0.88

Abbreviations: $AUC_{0\text{-}t\ hr}$, area under the curve-time curve from 0 to the time point, BA, bioavailability, PCTD, patch of cannabidiol loaded transdermal nanocarriers.

ratio of the surfactant in the nano carrier composition may not always lead to enhanced permeability of the carrier; conversely, it could impede the release of the drug or carrier due to interfacial interactions.[96–98] Additionally, the soft and hard segments in surfactants influences the micellar system, contingent upon the ratio of surfactants in the formulation, and has been demonstrated to affect the structural properties of the carrier, enhancing micellar packing, tuning mechanical properties, and improving interactions between oil and water interfaces.[99–102] In this study, CTD-12 chose materials such as Tween 80 (surfactants) and limonene (terpenes) as the main structural components of the nano carrier, which also served as penetration enhancers, facilitating carrier disruption of sebum, permeation through the stratum corneum, or across skin tissue layers. It is speculated that through the carrier design of CTD-12, the self-assembly characteristics enable it to maintain the shape and function of the nano carrier when penetrating the skin barrier, achieving better skin penetration through the tensile properties brought by the soft material and the lipid disturbance caused by the characteristics of the carrier material. The skin penetration data of CTD-41 (micelle system-like, containing more surfactant Tween 80) and CTD-12 (self-assembly system-like, containing less surfactant Tween 80) in this study further confirm this speculation. Once these nano-carriers breach the stratum corneum barrier and enter the epidermis and dermis tissues, the drug within the carrier can diffuse or be absorbed through various pathways, including intercellular, intracellular, and through follicular routes, ensuring effective drug delivery.[64,73,93,103] Furthermore, the endothelial cells of blood vessels and lymphatic vessels in the skin tissues served as pathways for the diffusion of drugs from the carrier into the bloodstream. Despite the size of nano-carriers hindering direct penetration into the vessels, CTD-12 still achieve enhanced drug bioavailability through optimized interactions, improved skin permeability, and effective drug delivery pathways.

Microneedle systems are widely believed to facilitate complete drug penetration through the stratum corneum, achieving optimal transdermal absorption.[104,105] In this study, it demonstrates that CTD-12 exhibits superior performance compared to previous CBD microneedle patents.[77] The reasons for this extend beyond differences in skin source and solution selection compared to patented technology. Notably, the patent under discussion relies on a conventional microneedle drug delivery system without incorporating nanocarrier technology. Instead, it directly employs CBD prodrug and CBD with microneedle patch technology. Traditional microneedle formulations have drawbacks, including the need for tailored design to match specific drug molecules, limited drug loading capacity, potential for skin allergies, and issues such as pore blockage or drug deposition at the application site.[106,107] Despite efforts to enhance microneedle systems and incorporate nanocarrier technology for next-generation transdermal drug delivery patches, the high production costs remain a significant challenge.[108–111] This study introduces the CTD-12 transdermal carrier formulation, tailored for CBD properties, as a cost-effective and easily scalable solution with excellent performance. Ultimately, both CTD-12 as a transdermal formulation and PCTD-12 as a drug patch demonstrate significant potential for future applications.

Conclusion

This study highlighted the promising attributes of CTD-12, a transdermal nanoparticle formulation, including small particle size, high encapsulation efficiency, and a favorable drug-loaded ratio for CBD. While demonstrating potential in drug patch systems, exploration of diverse patch formulations, such as oil gels or hydrogel systems, in tandem with CTD-12 was not undertaken in this study. Future research should focus on comprehensive bioavailability studies and diverse formulation combinations to advance CTD-12 development in TDDS. Overall, CTD-12 presented a promising transdermal delivery option for CBD, potentially improving treatment outcomes for various chronic diseases where CBD could be applied.

Abbreviations

CBD, cannabidiol; EE%, encapsulation efficiency; DL%, drug-loaded ratio; THC, tetrahydrocannabinol; TDDS, transdermal drug delivery system; SNEDDS, self-nanoemulsifying drug delivery systems; SLN, solid lipid nanoparticles; NLCs, nanostructured lipid carriers; DLS, dynamic light scattering; DAD, diode array detector; Oral, oral route; IV, intravenous injection; SRM, single reaction monitoring mode; PDI, Polydisperse Index; TD-NCs, Transdermal nanocarriers; CTD, Cannabidiol loaded transdermal nanocarriers; $AUC_{0\text{-}24hr}$, area under the curve-time curve from 0 to 24-hour time point; $Flux_{0\text{-}24hr}$, flux-time curve from 0 to 24-hour time point; FA, formulation bioavailability; BA, bioavailability; PCTD, patch of cannabidiol loaded transdermal nanocarriers.

Data Sharing Statement

The raw/processed data required to reproduce these findings cannot be shared at this time due to legal or ethical reasons.

Ethics Statements

The animal study was conducted according to the guidelines of the Animal Care Committee of the National Chung Hsing University and approved by the Committee (IACUC No. 111-127) and performed in accordance with the National Research Council's Guide for the Care and Use of Laboratory Animals.

Acknowledgments

This research was supported by grants from the Powin Biomedical Co., Ltd. of the Republic of China (R.O.C).

Funding

This research was funded by the Powin Biomedical Co., Ltd.

Disclosure

The authors declare no conflicts of interest.

References

1. Yu L, Madsen FB, Eriksen SH, Andersen AJC, Skov AL. A reliable quantitative method for determining CBD content and release from transdermal patches in Franz cells. *Phytochem Anal*. 2022;33(8):1257–1265. doi:10.1002/pca.3188
2. Gaston TE, Friedman D. Pharmacology of cannabinoids in the treatment of epilepsy. *Epilepsy Behav*. 2017;70:313–318. doi:10.1016/j.yebeh.2016.11.016
3. Huntsman RJ, Tang-Wai R, Shackelford AE. Cannabis for pediatric epilepsy. *J Clin Neurophysiol*. 2020;37(1):2–8. doi:10.1097/wnp.0000000000000641
4. Watt G, Karl T. In vivo evidence for therapeutic properties of cannabidiol (CBD) for Alzheimer's disease. *Front Pharmacol*. 2017;8:20. doi:10.3389/fphar.2017.00020
5. Crippa JA, Guimarães FS, Campos AC, Zuardi AW. Translational investigation of the therapeutic potential of cannabidiol (CBD): toward a new age. *Front Immunol*. 2018;9:2009. doi:10.3389/fimmu.2018.02009
6. Zuardi AW, Crippa JA, Hallak JE, et al. Cannabidiol for the treatment of psychosis in Parkinson's disease. *J Psychopharmacol*. 2009;23(8):979–983. doi:10.1177/0269881108096519
7. Shannon S, Lewis N, Lee H, Hughes S. Cannabidiol in anxiety and sleep: a large case series. *Perm J*. 2019;23:18–041. doi:10.7812/tpp/18-041
8. Chagas MH, Eckeli AL, Zuardi AW, et al. Cannabidiol can improve complex sleep-related behaviours associated with rapid eye movement sleep behaviour disorder in Parkinson's disease patients: a case series. *J Clin Pharm Ther*. 2014;39(5):564–566. doi:10.1111/jcpt.12179
9. García-Gutiérrez MS, Navarrete F, Gasparyan A, Austrich-Olivares A, Sala F, Manzanares J. Cannabidiol: a potential new alternative for the treatment of anxiety, depression, and psychotic disorders. *Biomolecules*. 2020;10(11):1575. doi:10.3390/biom10111575
10. McGuire P, Robson P, Cubala WJ, et al. Cannabidiol (CBD) as an adjunctive therapy in Schizophrenia: a multicenter randomized controlled trial. *Am J Psychiatry*. 2018;175(3):225–231. doi:10.1176/appi.ajp.2017.17030325
11. Millar SA, Maguire RF, Yates AS, O'Sullivan SE. Towards better delivery of cannabidiol (CBD). *Pharmaceuticals*. 2020;13(9):219. doi:10.3390/ph13090219
12. Hossain KR, Alghalayini A, Valenzuela SM. Current challenges and opportunities for improved cannabidiol solubility. *Int J Mol Sci*. 2023;24(19):14514. doi:10.3390/ijms241914514
13. Grifoni L, Vanti G, Donato R, Sacco C, Bilia AR. Promising nanocarriers to enhance solubility and bioavailability of cannabidiol for a plethora of therapeutic opportunities. *Molecules*. 2022;27(18):6070. doi:10.3390/molecules27186070
14. Millar SA, Stone NL, Yates AS, O'Sullivan SE. A systematic review on the pharmacokinetics of cannabidiol in humans. *Front Pharmacol*. 2018;9:1365. doi:10.3389/fphar.2018.01365
15. Huestis MA. Human cannabinoid pharmacokinetics. *Chem Biodivers*. 2007;4(8):1770–1804. doi:10.1002/cbdv.200790152
16. Kumeria T, Wang J, Kim B, et al. Enteric polymer-coated porous silicon nanoparticles for site-specific oral delivery of IgA antibody. *ACS Biomater Sci Eng*. 2022;8(10):4140–4152. doi:10.1021/acsbiomaterials.0c01313
17. Zhang Y, Wang Y, Li X, Nie D, Liu C, Gan Y. Ligand-modified nanocarriers for oral drug delivery: challenges, rational design, and applications. *J Control Release*. 2022;352:813–832. doi:10.1016/j.jconrel.2022.11.010
18. Ouyang J, Zhang Z, Deng B, et al. Oral drug delivery platforms for biomedical applications. *Mater*. 2023;62:296–326. doi:10.1016/j.mattod.2023.01.002
19. Durán-Lobato M, Niu Z, Alonso MJ. Oral delivery of biologics for precision medicine. *Adv Mater*. 2020;32(13):1901935. doi:10.1002/adma.201901935
20. Asad S, Jacobsen A-C, Teleki A. Inorganic nanoparticles for oral drug delivery: opportunities, barriers, and future perspectives. *Curr Opin Chem Eng*. 2022;38:100869. doi:10.1016/j.coche.2022.100869
21. Hyung Kang R, Hee Kim N, Kim D. A transformable and biocompatible polymer series using ring-opening polymerization of cyclic silane for more effective transdermal drug delivery. *Chem Eng J*. 2022;440:135989. doi:10.1016/j.cej.2022.135989

22. Li B, Lu G, Liu W, Liao L, Ban J, Lu Z. Formulation and evaluation of PLGA nanoparticulate-based microneedle system for potential treatment of neurological diseases. *Int J Nanomed*. 2023;18:3745–3760. doi:10.2147/ijn.S415728
23. Tanner EEL, Curreri AM, Balkaran JPR, et al. Design principles of Ionic liquids for transdermal drug delivery. *Adv Mater*. 2019;31 (27):1901103. doi:10.1002/adma.201901103
24. Hu H, Ruan H, Ruan S, et al. Acid-responsive PEGylated branching PLGA nanoparticles integrated into dissolving microneedles enhance local treatment of arthritis. *Chem Eng J*. 2022;431:134196. doi:10.1016/j.cej.2021.134196
25. Singh V, Kesharwani P. Recent advances in microneedles-based drug delivery device in the diagnosis and treatment of cancer. *J Control Release*. 2021;338:394–409. doi:10.1016/j.jconrel.2021.08.054
26. Prausnitz MR, Langer R. Transdermal drug delivery. *Nat Biotechnol*. 2008;26(11):1261–1268. doi:10.1038/nbt.1504
27. Chen Y, Wang M, Fang L. Biomaterials as novel penetration enhancers for transdermal and dermal drug delivery systems. *Drug Delivery*. 2013;20(5):199–209. doi:10.3109/10717544.2013.801533
28. Li H, Peng Z, Song Y, et al. Study of the permeation-promoting effect and mechanism of solid microneedles on different properties of drugs. *Drug Delivery*. 2023;30(1):2165737. doi:10.1080/10717544.2023.2165737
29. Zhao W, Zheng L, Yang J, Ma Z, Tao X, Wang Q. Dissolving microneedle patch-assisted transdermal delivery of methotrexate improve the therapeutic efficacy of rheumatoid arthritis. *Drug Delivery*. 2023;30(1):121–132. doi:10.1080/10717544.2022.2157518
30. Jamaledin R, Yiu CKY, Zare EN, et al. Advances in antimicrobial microneedle patches for combating infections. *Adv Mater*. 2020;32 (33):2002129. doi:10.1002/adma.202002129
31. Adin SN, Gupta I, Rashid MA, Alhamhoom Y, Aqil M, Mujeeb M. Nanotransethosomes for enhanced transdermal delivery of mangiferin against rheumatoid arthritis: formulation, characterization, invivo pharmacokinetic and pharmacodynamic evaluation. *Drug Delivery*. 2023;30 (1):2173338. doi:10.1080/10717544.2023.2173338
32. Qindeel M, Ullah MH, Fakhar Ud D, Ahmed N, Rehman A. Recent trends, challenges and future outlook of transdermal drug delivery systems for rheumatoid arthritis therapy. *J Control Release*. 2020;327:595–615. doi:10.1016/j.jconrel.2020.09.016
33. Yu P, Zhang X, Cheng G, et al. Construction of a new multifunctional insomnia drug delivery system. *Chem Eng J*. 2022;430:132633. doi:10.1016/j.cej.2021.132633
34. Yang H, Mu W, Wei D, et al. A novel targeted and high-efficiency nanosystem for combinational therapy for Alzheimer's disease. *Adv Sci*. 2020;7(19):1902906. doi:10.1002/advs.201902906
35. Fattahi N, Shahbazi M-A, Maleki A, Hamidi M, Ramazani A, Santos HA. Emerging insights on drug delivery by fatty acid mediated synthesis of lipophilic prodrugs as novel nanomedicines. *J Control Release*. 2020;326:556–598. doi:10.1016/j.jconrel.2020.07.012
36. Sun J, Wei C, Liu Y, et al. Progressive release of mesoporous nano-selenium delivery system for the multi-channel synergistic treatment of Alzheimer's disease. *Biomaterials*. 2019;197:417–431. doi:10.1016/j.biomaterials.2018.12.027
37. Liu Y, Shen J, Shi J, et al. Functional polymeric core–shell hybrid nanoparticles overcome intestinal barriers and inhibit breast cancer metastasis. *Chem Eng J*. 2022;427:131742. doi:10.1016/j.cej.2021.131742
38. Mou Y, Zhang P, Lai W-F, Zhang D. Design and applications of liposome-in-gel as carriers for cancer therapy. *Drug Delivery*. 2022;29 (1):3245–3255. doi:10.1080/10717544.2022.2139021
39. Srivastav AK, Karpathak S, Rai MK, Kumar D, Misra DP, Agarwal V. Lipid based drug delivery systems for oral, transdermal and parenteral delivery: recent strategies for targeted delivery consistent with different clinical application. *J Drug Deliv Sci Technol*. 2023;85:104526. doi:10.1016/j.jddst.2023.104526
40. Kansız S, Elçin YM. Advanced liposome and polymersome-based drug delivery systems: considerations for physicochemical properties, targeting strategies and stimuli-sensitive approaches. *Adv Colloid Interface Sci*. 2023;102930. doi:10.1016/j.cis.2023.102930
41. Spleis H, Sandmeier M, Claus V, Bernkop-Schnürch A. Surface design of nanocarriers: key to more efficient oral drug delivery systems. *Adv Colloid Interface Sci*. 2023;313:102848. doi:10.1016/j.cis.2023.102848
42. Battistella C, Liang Y, Gianneschi NC. Innovations in disease state responsive soft materials for targeting extracellular stimuli associated with cancer, cardiovascular disease, diabetes, and beyond. *Adv Mater*. 2021;33(46):2007504. doi:10.1002/adma.202007504
43. Li M, Li M, Li X, et al. Preparation, characterization and ex vivo skin permeability evaluation of type I collagen-loaded liposomes. *Int J Nanomed*. 2023;18:1853–1871. doi:10.2147/ijn.S404494
44. Hassan AS, Hofni A, Abourehab MAS, Abdel-Rahman IAM. Ginger extract-loaded transethosomes for effective transdermal permeation and anti-inflammation in rat model. *Int J Nanomed*. 2023;18:1259–1280. doi:10.2147/ijn.S400604
45. Constantinou AP, Tall A, Li Q, Georgiou TK. Liquid–liquid phase separation in aqueous solutions of poly(ethylene glycol) methacrylate homopolymers. *J Polym Sci*. 2022;60(2):188–198. doi:10.1002/pol.20210714
46. Mandrioli M, Tura M, Scotti S, Gallina Toschi T. Fast detection of 10 cannabinoids by RP-HPLC-UV method in cannabis sativa l. *Molecules*. 2019;24(11). doi:10.3390/molecules24112113
47. Citti C, Pacchetti B, Vandelli MA, Forni F, Cannazza G. Analysis of cannabinoids in commercial hemp seed oil and decarboxylation kinetics studies of cannabidiolic acid (CBDA). *J Pharm Biomed Anal*. 2018;149:532–540. doi:10.1016/j.jpba.2017.11.044
48. Opuni KFM, Boadu JA, Amponsah SK, Okai CA. High performance liquid chromatography: a versatile tool for assaying antiepileptic drugs in biological matrices. *J Chromatogr B*. 2021;1179:122750. doi:10.1016/j.jchromb.2021.122750
49. Uchida T, Kadhum WR, Kanai S, Todo H, Oshizaka T, Sugibayashi K. Prediction of skin permeation by chemical compounds using the artificial membrane, Strat-M™. *Eur J Pharm Sci*. 2015;67:113–118. doi:10.1016/j.ejps.2014.11.002
50. Wang C, Wang J, Sun Y, et al. Enhanced stability and oral bioavailability of cannabidiol in zein and whey protein composite nanoparticles by a modified anti-solvent approach. *Foods*. 2022;11(3). doi:10.3390/foods11030376
51. Ujváry I, Hanuš L. Human metabolites of cannabidiol: a review on their formation, biological activity, and relevance in therapy. *Cannabis Cannabinoid Res*. 2016;1(1):90–101. doi:10.1089/can.2015.0012
52. Pichini S, Malaca S, Gottardi M, et al. UHPLC-MS/MS analysis of cannabidiol metabolites in serum and urine samples. application to an individual treated with medical cannabis. *Talanta*. 2021;223:121772. doi:10.1016/j.talanta.2020.121772
53. Meng Q, Buchanan B, Zuccolo J, Poulin -M-M, Gabriele J, Baranowski DC. A reliable and validated LC-MS/MS method for the simultaneous quantification of 4 cannabinoids in 40 consumer products. *PLoS One*. 2018;13(5):e0196396. doi:10.1371/journal.pone.0196396

54. Manca A, Chiara F, Mula J, et al. A new UHPLC-MS/MS method for cannabinoids determination in human plasma: a clinical tool for therapeutic drug monitoring. *Biomed Pharmacother*. 2022;156:113899. doi:10.1016/j.biopha.2022.113899
55. Citti C, Linciano P, Panseri S, et al. Cannabinoid profiling of hemp seed oil by liquid chromatography coupled to high-resolution mass spectrometry. *Original Research Front Plant Sci*. 2019;2019:10. doi:10.3389/fpls.2019.00120
56. Palazzoli F, Citti C, Licata M, et al. Development of a simple and sensitive liquid chromatography triple quadrupole mass spectrometry (LC–MS/MS) method for the determination of cannabidiol (CBD), Δ9-tetrahydrocannabinol (THC) and its metabolites in rat whole blood after oral administration of a single high dose of CBD. *J Pharm Biomed Anal*. 2018;150:25–32. doi:10.1016/j.jpba.2017.11.054
57. Deiana S, Watanabe A, Yamasaki Y, et al. Plasma and brain pharmacokinetic profile of cannabidiol (CBD), cannabidivarine (CBDV), Δ^9-tetrahydrocannabivarin (THCV) and cannabigerol (CBG) in rats and mice following oral and intraperitoneal administration and CBD action on obsessive-compulsive behaviour. *Psychopharmacology*. 2012;219(3):859–873. doi:10.1007/s00213-011-2415-0
58. Cherniakov I, Izgelov D, Domb AJ, Hoffman A. The effect of Pro nanolipospheres (PNL) formulation containing natural absorption enhancers on the oral bioavailability of delta-9-tetrahydrocannabinol (THC) and cannabidiol (CBD) in a rat model. *Eur J Pharm Sci*. 2017;109:21–30. doi:10.1016/j.ejps.2017.07.003
59. Williams AC, Barry BW. Penetration enhancers. *Adv Drug Deliv Rev*. 2012;64:128–137. doi:10.1016/j.addr.2012.09.032
60. Dragicevic-Curic N, Scheglmann D, Albrecht V, Fahr A. Temoporfin-loaded invasomes: development, characterization and in vitro skin penetration studies. *J Control Release*. 2008;127(1):59–69. doi:10.1016/j.jconrel.2007.12.013
61. Waheed A, Aqil M, Ahad A, et al. Improved bioavailability of raloxifene hydrochloride using limonene containing transdermal nano-sized vesicles. *J Drug Deliv Sci Technol*. 2019;52:468–476. doi:10.1016/j.jddst.2019.05.019
62. Lu B, Bo Y, Yi M, et al. Enhancing the solubility and transdermal delivery of drugs using ionic liquid-In-oil microemulsions. *Adv Funct Mater*. 2021;31(34):2102794. doi:10.1002/adfm.202102794
63. Cappel MJ, Kreuter J. Effect of nonionic surfactants on transdermal drug delivery: i. Polysorbates. *Int J Pharm*. 1991;69(2):143–153. doi:10.1016/0378-5173(91)90219-E
64. Phatale V, Vaiphei KK, Jha S, Patil D, Agrawal M, Alexander A. Overcoming skin barriers through advanced transdermal drug delivery approaches. *J Control Release*. 2022;351:361–380. doi:10.1016/j.jconrel.2022.09.025
65. Zhu Y, Xu W, Zhang J, et al. Self-microemulsifying Drug Delivery System for Improved Oral Delivery of Limonene: preparation, Characterization, in vitro and in vivo Evaluation. *AAPS Pharm Sci Tech*. 2019;20(4):153. doi:10.1208/s12249-019-1361-8
66. W-C L, Chiang B-H, Huang D-W, P-H L. Skin permeation of d-limonene-based nanoemulsions as a transdermal carrier prepared by ultrasonic emulsification. *Ultrason Sonochem*. 2014;21(2):826–832. doi:10.1016/j.ultsonch.2013.10.013
67. Juang R-S, Lin K-H. Ultrasound-assisted production of W/O emulsions in liquid surfactant membrane processes. *Colloids Surf a Physicochem Eng Asp*. 2004;238(1):43–49. doi:10.1016/j.colsurfa.2004.02.028
68. Capek I. Degradation of kinetically-stable o/w emulsions. *Adv Colloid Interface Sci*. 2004;107(2):125–155. doi:10.1016/S0001-8686(03)00115-5
69. Haq A, Goodyear B, Ameen D, Joshi V, Michniak-Kohn B. Strat-M® synthetic membrane: permeability comparison to human cadaver skin. *Int J Pharm*. 2018;547(1):432–437. doi:10.1016/j.ijpharm.2018.06.012
70. Bolla PK, Clark BA, Juluri A, Cheruvu HS, Renukuntla J. Evaluation of formulation parameters on permeation of Ibuprofen from topical formulations using Strat-M® membrane. *Pharmaceutics*. 2020;12(2):151. doi:10.3390/pharmaceutics12020151
71. Czajkowska-Kośnik A, Szymańska E, Winnicka K. Nanostructured lipid carriers (NLC)-based gel formulations as etodolac delivery: from gel preparation to permeation study. *Molecules*. 2023;28(1). doi:10.3390/molecules28010235
72. Pulsoni I, Lubda M, Aiello M, et al. Comparison between Franz diffusion cell and a novel micro-physiological system for in vitro penetration assay using different skin models. *SLAS Technol*. 2022;27(3):161–171. doi:10.1016/j.slast.2021.12.006
73. Shukla T, Upmanyu N, Agrawal M, Saraf S, Saraf S, Alexander A. Biomedical applications of microemulsion through dermal and transdermal route. *Biomed Pharmacother*. 2018;108:1477–1494. doi:10.1016/j.biopha.2018.10.021
74. Stinchcomb Audra L, Banks SL; inventors; ALLTRANZ INC, assignee. Formulations of cannabidiol and prodrugs of cannabidiol and methods of using the same. US patent US 2010/0273895 A1. patent application US 76951910 A. 2010.
75. Stinchcomb Audra L, Banks SL; inventors; ALLTRANZ INC, assignee. Transdermal formulations of cannabidiol comprising a penetration enhancer and methods of using the same. CA patent CA 2760460 C. patent application CA 2760460 A; 2019.
76. Stinchcomb Audra L, Nalluri Buchi N; Inventors; STINCHCOMB AUDRA L, NALLURI BUCHI N, ALLTRANZ LLC, assignee. Transdermal delivery of cannabidiol. US patent US 8435556 B2. patent application US 51122609 A; 2013.
77. Stinchcomb Audra L, Banks SL, Golinski Miroslaw J, Howard Jeffery L, Hammell Dana C; inventors ZYNERBA PHARMACEUTICALS INC, assignee. Use of cannabidiol prodrugs in topical and transdermal administration with microneedles. US patent US 9533942 B2. patent application US 201414539824 A; 2017.
78. Morakul B, Junyaprasert VB, Sakchaisri K, Teeranachaideekul V. Cannabidiol-Loaded Nanostructured Lipid Carriers (NLCs) for Dermal Delivery: enhancement of Photostability, Cell Viability, and Anti-Inflammatory Activity. *Pharmaceutics*. 2023;15(2):537. doi:10.3390/pharmaceutics15020537
79. Franzè S, Angelo L, Casiraghi A, Minghetti P, Cilurzo F. Design of Liposomal Lidocaine/Cannabidiol Fixed Combinations for Local Neuropathic Pain Treatment. *Pharmaceutics*. 2022;14(9):1915. doi:10.3390/pharmaceutics14091915
80. Franzè S, Ricci C, Del Favero E, Rama F, Casiraghi A, Cilurzo F. Micelles-in-liposome systems obtained by proliposomal approach for cannabidiol delivery: structural features and skin penetration. *Mol Pharm*. 2023;20(7):3393–3402. doi:10.1021/acs.molpharmaceut.3c00044
81. Demisli S, Galani E, Goulielmaki M, et al. Encapsulation of cannabidiol in oil-in-water nanoemulsions and nanoemulsion-filled hydrogels: a structure and biological assessment study. *J Colloid Interface Sci*. 2023;634:300–313. doi:10.1016/j.jcis.2022.12.036
82. Sharkawy A, Silva AM, Rodrigues F, Barreiro F, Rodrigues A. Pickering emulsions stabilized with chitosan/collagen peptides nanoparticles as green topical delivery vehicles for cannabidiol (CBD). *Colloids Surf a Physicochem Eng Asp*. 2021;631:127677. doi:10.1016/j.colsurfa.2021.127677
83. Pimenta AFR, Vieira AP, Colaço R, et al. Controlled release of moxifloxacin from intraocular lenses modified by Ar plasma-assisted grafting with AMPS or SBMA: an in vitro study. *Colloids Surf B*. 2017;156:95–103. doi:10.1016/j.colsurfb.2017.04.060

84. Naeem A, Yu C, Liu Y, Feng Y, Fan J, Guan Y. Study of Gelatin-grafted-2-Acrylamido-2-methylpropane sulfonic acid hydrogels as a controlled release vehicle for amorphous solid dispersion of Tripterygium Wilfordii bioactive constituents. *Arab J Chem*. 2023;16(10):105139. doi:10.1016/j.arabjc.2023.105139
85. Cheng F-M, Chen H-X, Li H-D. Recent advances in tough and self-healing nanocomposite hydrogels for shape morphing and soft actuators. *Eur Polym J*. 2020;124:109448. doi:10.1016/j.eurpolymj.2019.109448
86. Brookes A, Jewell A, Feng W, Bradshaw TD, Butler J, Gershkovich P. Oral lipid-based formulations alter delivery of cannabidiol to different anatomical regions in the brain. *Int J Pharm*. 2023;635:122651. doi:10.1016/j.ijpharm.2023.122651
87. Zgair A, Wong JCM, Sabri A, et al. Development of a simple and sensitive HPLC–UV method for the simultaneous determination of cannabidiol and Δ9-tetrahydrocannabinol in rat plasma. *J Pharm Biomed Anal*. 2015;114:145–151. doi:10.1016/j.jpba.2015.05.019
88. Siemens AJ, Walczak D, Buckley FE. Characterization of blood disappearance and tissue distribution of [3H]cannabidiol. *Biochem Pharmacol*. 1980;29(3):462–464. doi:10.1016/0006-2952(80)90532-8
89. Muresan P, Woodhams S, Smith F, et al. Evaluation of cannabidiol nanoparticles and nanoemulsion biodistribution in the central nervous system after intrathecal administration for the treatment of pain. *Nanomedicine*. 2023;49:102664. doi:10.1016/j.nano.2023.102664
90. Beal R, Fitzsimmons N, McMahon A, Sand B, Martinez K; inventors; AMPERSAND BIOPHARMACEUTICALS INC, assignee. Transdermal penetrant formulations containing cannabidiol. US patent US 10842758 B1. patent application US 201916546269 A; 2020.
91. Fitzsimmons N, Beal R, McMahon A, Sand B, Martinez K; Inventors; AMPERSAND BIOPHARMACEUTICALS INC, DYVE BIOSCIENCES INC, assignee. Transdermal penetrant formulations containing cannabidiol. US patent US 11026896 B2. patent application US 201916546270 A; 2021.
92. Fitzsimmons N, Beal R, McMahon A, Sand B, Martinez K; Inventors; DYVE BIOSCIENCES INC, assignee. Transdermal penetrant formulations containing cannabidiol. US patent US 2023/0038462 A1. patent application US 202017422434 A; 2023.
93. Khan SU, Ullah M, Saeed S, et al. Nanotherapeutic approaches for transdermal drug delivery systems and their biomedical applications. *Eur Polym J*. 2024;207:112819. doi:10.1016/j.eurpolymj.2024.112819
94. Leong MY, Kong YL, Burgess K, Wong WF, Sethi G, Looi CY. Recent Development of Nanomaterials for Transdermal Drug Delivery. *Biomedicines*. 2023;11(4):1124. doi:10.3390/biomedicines11041124
95. Münch S, Wohlrab J, Neubert RHH. Dermal and transdermal delivery of pharmaceutically relevant macromolecules. *Eur J Pharm Biopharm*. 2017;119:235–242. doi:10.1016/j.ejpb.2017.06.019
96. Heuschkel S, Goebel A, Neubert RHH. Microemulsions—modern colloidal carrier for dermal and transdermal drug delivery. *J Pharmaceut Sci*. 2008;97(2):603–631. doi:10.1002/jps.20995
97. Sintov AC, Shapiro L. New microemulsion vehicle facilitates percutaneous penetration in vitro and cutaneous drug bioavailability in vivo. *J Control Release*. 2004;95(2):173–183. doi:10.1016/j.jconrel.2003.11.004
98. Yuan Y, S-m L, F-k M, D-f Z. Investigation of microemulsion system for transdermal delivery of meloxicam. *Int J Pharm*. 2006;321(1):117–123. doi:10.1016/j.ijpharm.2006.06.021
99. Obradović S, Poša M. The influence of the structure of selected Brij and Tween homologues on the thermodynamic stability of their binary mixed micelles. *J Chem Thermodyn*. 2017;110:41–50. doi:10.1016/j.jct.2017.01.020
100. Ćirin D, Krstonošić V, Poša M. Properties of poloxamer 407 and polysorbate mixed micelles: influence of polysorbate hydrophobic chain. *J Ind Eng Chem*. 2017;47:194–201. doi:10.1016/j.jiec.2016.11.032
101. Wang X, Gao Y. Effects of length and unsaturation of the alkyl chain on the hydrophobic binding of curcumin with Tween micelles. *Food Chem*. 2018;246:242–248. doi:10.1016/j.foodchem.2017.11.024
102. Chen S-Y, Kokalari I, Parnell SR, et al. Structure property relationship of micellar waterborne poly(urethane-urea): tunable mechanical properties and controlled release profiles with amphiphilic triblock copolymers. *Langmuir*. 2023;39(29):10033–10046. doi:10.1021/acs.langmuir.3c00921
103. Alkilani AZ, McCrudden MT, Donnelly RF. Transdermal Drug Delivery: innovative Pharmaceutical Developments Based on Disruption of the Barrier Properties of the stratum corneum. *Pharmaceutics*. 2015;7(4):438–470. doi:10.3390/pharmaceutics7040438
104. Mo R, Zhang H, Xu Y, et al. Transdermal drug delivery via microneedles to mediate wound microenvironment. *Adv Drug Deliv Rev*. 2023;195:114753. doi:10.1016/j.addr.2023.114753
105. Yang D, Chen M, Sun Y, et al. Microneedle-mediated transdermal drug delivery for treating diverse skin diseases. *Acta Biomater*. 2021;121:119–133. doi:10.1016/j.actbio.2020.12.004
106. Sabbagh F, Kim BS. Recent advances in polymeric transdermal drug delivery systems. *J Control Release*. 2022;341:132–146. doi:10.1016/j.jconrel.2021.11.025
107. An H, Gu Z, Huang Z, et al. Novel microneedle platforms for the treatment of wounds by drug delivery: a review. *Colloids Surf B*. 2024;233:113636. doi:10.1016/j.colsurfb.2023.113636
108. Zheng L, Chen Y, Gu X, et al. Co-delivery of drugs by adhesive transdermal patches equipped with dissolving microneedles for the treatment of rheumatoid arthritis. *J Control Release*. 2024;365:274–285. doi:10.1016/j.jconrel.2023.11.029
109. Liu R, Li A, Lang Y, et al. Stimuli-responsive polymer microneedles: a rising transdermal drug delivery system and Its applications in biomedical. *J Drug Deliv Sci Technol*. 2023;88:104922. doi:10.1016/j.jddst.2023.104922
110. Sartawi Z, Blackshields C, Faisal W. Dissolving microneedles: applications and growing therapeutic potential. *J Control Release*. 2022;348:186–205. doi:10.1016/j.jconrel.2022.05.045
111. Zhang X, Hasani-Sadrabadi MM, Zarubova J, et al. Immunomodulatory microneedle patch for periodontal tissue regeneration. *Matter*. 2022;5(2):666–682. doi:10.1016/j.matt.2021.11.017

International Journal of Nanomedicine Dovepress

Publish your work in this journal

The International Journal of Nanomedicine is an international, peer-reviewed journal focusing on the application of nanotechnology in diagnostics, therapeutics, and drug delivery systems throughout the biomedical field. This journal is indexed on PubMed Central, MedLine, CAS, SciSearch®, Current Contents®/Clinical Medicine, Journal Citation Reports/Science Edition, EMBase, Scopus and the Elsevier Bibliographic databases. The manuscript management system is completely online and includes a very quick and fair peer-review system, which is all easy to use. Visit http://www.dovepress.com/testimonials.php to read real quotes from published authors.

Submit your manuscript here: https://www.dovepress.com/international-journal-of-nanomedicine-journal